Semiconductors, 2022, Vol. 56, No. 12

On the effect of etching with a focused Ga^+ ion beam in the energy range 12–30 keV on the luminescent properties of the $Al_{0.18}Ga_{0.82}As/GaAs/Al_{0.18}Ga_{0.82}As$ heterostructure

© G.V. Voznyuk[1,2], I.N. Grigorenko[1,2], A.S. Lila[2], M.I. Mitrofanov[1,3], D.N. Nikolaev[1], V.P. Evtikhiev[1,2]

[1] Ioffe Institute,
194021 St. Petersburg, Russia
[2] ITMO University,
197101 St. Petersburg, Russia
[3] Submicron Heterostructures for Microelectronics, Research and Engineering Center,
Russian Academy of Sciences,
194021 St. Petersburg, Russia
E-mail: glebufa0@gmail.come

Received December 8, 2022
Revised December 12, 2022
Accepted December 12, 2022

The effect of ion energy in a focused ion beam in the range 12–30 keV on the formation depth of nonradiative recombination centers during etching of the $Al_{0.18}Ga_{0.82}As/GaAs/Al_{0.18}Ga_{0.82}As$ double heterostructure has been studied. It is shown that an increase in the ion energy leads to an increase in the concentration and propagation depth of radiation defects. It was found that during etching of focused ion beam with ion energies above 15 keV, the depth of formation of radiation defects exceeds 900 nm, which does not correspond to the calculations in the Stopping and Range of Ions in Matter.

Keywords: focused ion beam, radiation defects, photoluminescence, annealing, AlGaAs/GaAs.

DOI: 10.21883/SC.2022.12.55147.4423

1. Introduction

The method of focused ion-beam (FIB) etching is traditionally used for preparation of samples for transmission electron microscopy (TEM) [1], local analysis, etching and deposition of materials [2], and fabrication of probes for atomic force microscopy (AFM) [3].

Focused ion beams are currently being used more and more often to fabricate nanophotonic elements. The specific features of ion-beam lithography (direct maskless patterning, high spatial resolution, potential to form patterns on nonplanar surfaces) provide an opportunity to design and modify devices with submicrometer nanophotonic elements (Bragg gratings [4], photonic crystals [5]).

The primary factor limiting the application of FIB lithography to light-emitting structures is the formation of radiation defects, which serve as nonradiative recombination centers [6], in the process of etching. However, the influence of major ion beam parameters (energy, current density, irradiation time) on the concentration and the spatial distribution of nonradiative recombination centers remains understudied.

In the present study, we report the results of examination of influence of Ga^+ FIBs with an ion energy within the 12–30 keV range on the depth of formation of nonradiative recombination centers in the process of etching of an $Al_{0.18}Ga_{0.82}As/GaAs/Al_{0.18}Ga_{0.82}As$ double heterostructure.

2. Experiment

An $Al_{0.18}Ga_{0.82}As/GaAs/Al_{0.18}Ga_{0.82}As$ double heterostructure with each of its layers being 1-μm-thick was examined. It was chosen to be studied for the fact that $Al_{0.18}Ga_{0.82}As$ barrier layers allowed us to investigate the luminescence of a GaAs potential well under its direct photoexcitation, and the GaAs layer thickness (1 μm) provided efficient absorption of radiation of a laser operating at a wavelength of 808 nm. Square apertures $100 \times 100\,\mu$m in size were formed on the structure surface by FIB etching under normal incidence of a beam with Ga^+ ion energies of 15–30 keV. The influence of radiation damage was estimated by monitoring the variation of luminescence intensity with depth of etched apertures. Ion-beam lithography was performed using an ultrahigh-vacuum FIB-SEM setup fitted with ion (COBRA) and electron (e-CLIPSE Plus) columns produced by Orsay Physics. A liquid-metal source of Ga^+ ions was used. The ion energy was varied within the 15–30 keV range with a pitch of 5 keV. To prevent the formation of gallium droplets on the structure surface, etching was performed with the use of a XeF_2 precursor.

3. Results and discussion

The influence of ion energy on the rate of etching of the $Al_{0.18}Ga_{0.82}As/GaAs/Al_{0.18}Ga_{0.82}As$ structure was estimated first. A test set of square apertures $5 \times 5\,\mu$m

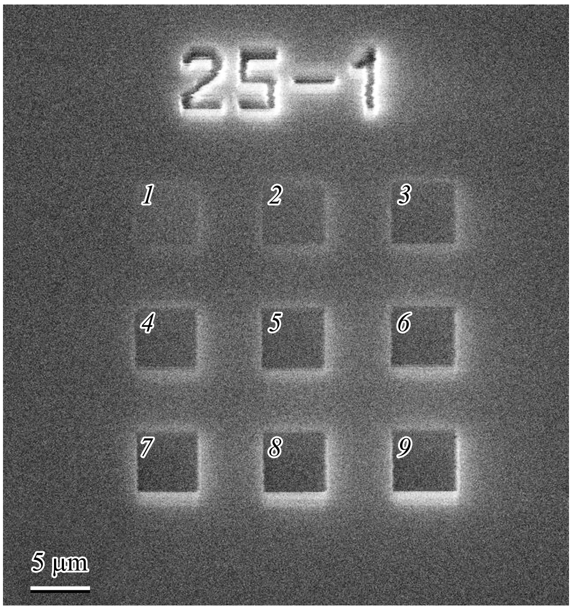

Figure 1. SEM image of one of the arrays of square apertures formed by an FIB with an ion energy of 25 keV. The depth increases smoothly from the first aperture to the ninth one.

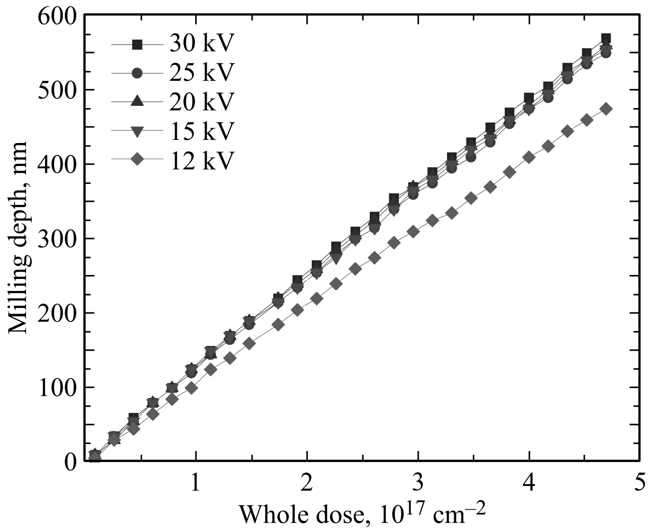

Figure 2. Dependence of the etching depth on the ion dose in FIB etching with different ion energies.

in size was etched by direct Ga^+ FIB lithography with ion energies of 12, 15, 20, 25, and 30 keV. The working beam current was 1 nA. Apertures grow deeper due to an increase in the ion dose achieved by increasing the number of exposures. Figure 1 shows the test lithographic pictures imaged with a scanning electron microscope (SEM).

The etching depth was measured with an NTMDT Solver Pro AFM. Figure 2 presents dependences of the depth of apertures on the ion dose for ion energies of 12, 15, 20, 25, and 30 keV in the beam. As the ion energy varies from 15 to 30 keV, the depth of apertures remains the same; therefore, the etching rate also remains unchanged. When the ion energy drops to 12 keV, the etching rate decreases by a factor of ~ 1.15.

Saturation of the etching rate with an increase in the ion energy has been observed earlier in [7]. In accordance with the model of the process developed in [8], the displacement of surface and near-surface atoms from their equilibrium positions becomes energetically possible as soon as the energy of sputtering ions exceeds the surface binding energy of the target material. These displaced atoms induce repulsive collisions, which eventually lead to ejection of atoms (recoil atoms) from the target surface. This energy range is specific in that the sputtering yield (0.1–3.0 for most materials) depends approximately linearly on the energy of bombarding ions and the ion current. Cascade-collisional (nonlinear cascade) sputtering is observed at ion energies above the threshold of ≈ 1 keV. The energy of Incident ions in this regime is sufficient to displace several target atoms, while the sputtering yields fall within the range from 5 to 50 (and may be even greater). A further increase in the energy of bombarding ions leads to deep ion implantation, the energy of recoil atoms dissipates within the bulk of the structure, and the yield factor reaches saturation (or even decreases).

To study photoluminescence, a set of square apertures $100 \times 100\,\mu$m in size was etched to a depth of 100 nm in the same structure by a focused beam of Ga^+ ions with energies of 15, 20, 25, and 30 keV. The ion dose was 10^{17} cm^{-2} in all cases. Owing to the instability of operating ion current in etching at an ion energy of 12 keV, the luminescence of these samples was not measured.

Etched samples were annealed for 20 min at a temperature of 300°C. This annealing regime provides an opportunity to remove the amorphized surface layer without recovery of radiation defects [9,10]. Photoluminescence was excited by a semiconductor laser operating at a wavelength of 808 nm with a spot diameter of $80\,\mu$m directly in the active GaAs layer of the $Al_{0.18}Ga_{0.82}As/GaAs/Al_{0.18}Ga_{0.82}As$ heterostructure. The photoexcitation power density was 1.5 kW/cm^2. Photoluminescence spectra contained only the edge luminescence line of GaAs with a FWHM of 40 meV. The luminescence intensity was estimated by measuring the spectrum area. Figure 3 shows the dependence of photoluminescence intensity, which is normalized to the intensity corresponding to the unetched sample part, on the ion energy.

The intensity of luminescence from apertures etched by an FIB with an ion energy of 15 keV is roughly the same as the intensity of luminescence of the unetched sample. When the FIB ion energy increases to 30 keV, the luminescence intensity decreases almost by a factor of 3. With sub-barrier direct photoexcitation, the observed GaAs luminescence intensity reduction in the active region of the $Al_{0.18}Ga_{0.82}As/GaAs/Al_{0.18}Ga_{0.82}As$ heterostructure is feasible only if nonradiative recombination centers form in the GaAs layer. In order to analyze the obtained dependences, we calculated the spatial distribution of

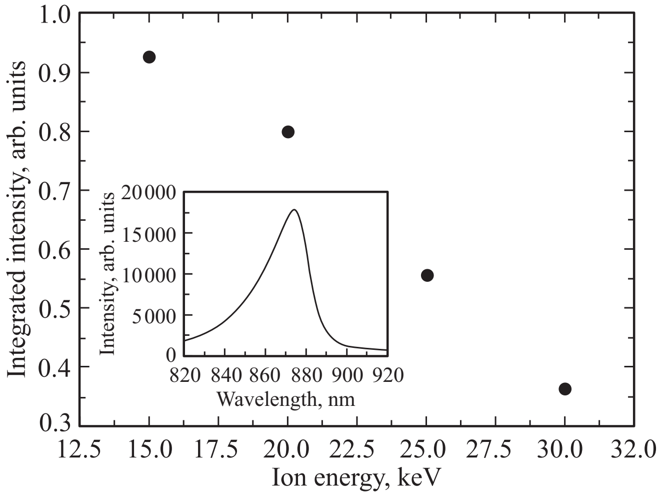

Figure 3. Relative integrated photoluminescence intensity as a function of the in energy. The photoluminescence spectrum from the region of the $Al_{0.18}Ga_{0.82}As/GaAs/Al_{0.18}Ga_{0.82}As$ heterostructure etched by ions with an energy of 30 keV is shown in the inset.

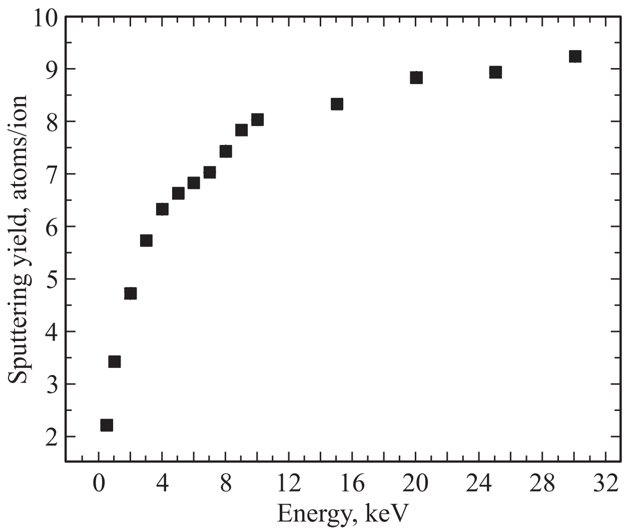

Figure 4. Calculated dependence of the $Al_{0.18}Ga_{0.82}As$ sputtering yield on the energy of Ga^+ ions.

radiation defects and the number of etched atoms per ion (sputtering yield) in SRIM (Stopping and Range of Ions in Matter). The calculated dependence of the sputtering yield (Fig. 4) verifies the experimental data: the etching rate increases with ion energy and reaches saturation at an energy of ~ 12 keV.

The calculated distribution of the reduced overall number of Al, Ga, and As vacancies over the $Al_{0.18}Ga_{0.82}As$ layer thickness for ion energies of 5−30 keV is presented in Fig. 5, *a*. Figure 5, *b* shows the dependence of the reduced overall number of Al, Ga, and As vacancies in the $Al_{0.18}Ga_{0.82}As$ layer at a distance of 30 nm from the etching front.

The number of vacancies increases markedly with ion energy in a focused ion beam. Since the Shockley–Read–Hall nonradiative recombination rate is related linearly to the concentration of nonradiative recombination centers, it may be concluded that the results of calculations agree qualitatively with the measured luminescence intensity reduction. Note that the experiment reveals a several-fold greater depth of formation of radiation defects. When 1-μm-thick $Al_{0.18}Ga_{0.82}As$ is etched to a depth of just 100 nm by an ion beam with an energy of 30 keV, the luminescence intensity decreases by a factor of 3 relative to the intensity of luminescence of the region etched by an FIB with an energy of 15 keV. The concentration of vacancies at the $Al_{0.18}Ga_{0.82}As/GaAs$ heterointerface (900 nm from the etching front) estimated based on the calculated (SRIM) spatial distribution of the overall number of vacancies (Fig. 5, *a*) and the experimental fluence value is negligible.

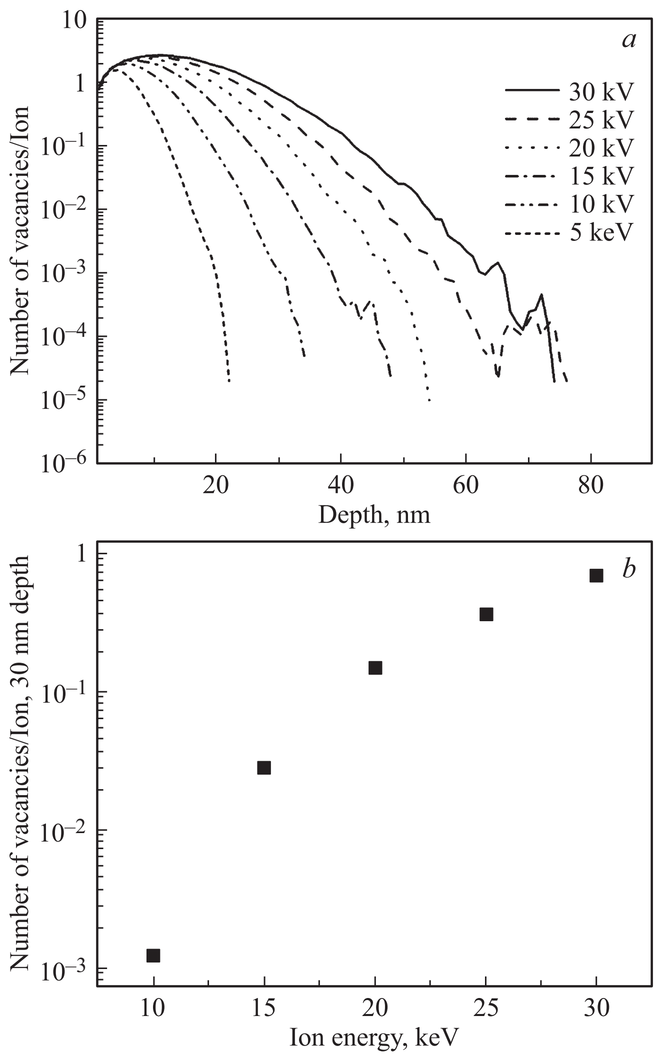

Figure 5. Results of numerical calculations in SRIM: *a* — spatial distribution of the reduced overall number of Al, Ga, As vacancies in the $Al_{0.18}Ga_{0.82}As$ layer; *b* — reduced overall number of vacancies per ion at a distance of 30 nm from the etching front as a function of the ion energy.

The observed difference between experimental and calculated data could potentially be attributed to the diffusion of vacancies stimulated by overheating of the sample. However, the presence of a surface layer amorphized due to etching suggests that no overheating $> 100^\circ$C was induced [11]. The other probable reasons behind the discrepancy between calculated and experimental data include the neglect of overlap of collision cascades [12] in SRIM and the channeling effect [13]. Additional studies of the dependence of the defect formation depth on the angle of incidence of a focused ion beam are needed to examine the possible influence of channeling.

4. Conclusion

The obtained results revealed that the rate of etching of $Al_{0.18}Ga_{0.82}As$ layers is virtually independent of the ion energy in a focused ion beam within the energy range of 15–30 keV. At the same time, the depth of formation of radiation defects increases rapidly with Ga^+ ion energy. It was found that this depth exceeds 900 nm in the case of etching by FIBs with ion energies higher than 15 keV. This contradicts the results of calculations in SRIM. Thus, ion energies < 15 keV are better suited for direct ion-beam patterning of light-emitting structures by a focused Ga^+ ion beam than the traditionally used energies of 20–30 keV.

Funding

Photoluminescence measurements and the processing of their results performed by V.P. Evtikhiev and I.N. Grigorenko (ITMO University) were supported financially by grant No. 21-12-00304 from the Russian Science Foundation, https://rscf.ru/project/21-12-00304/. The analysis of parameters of lithographic picture etching performed by G.V. Voznyuk (ITMO University) was supported financially by grant No 20-79-10285 from the Russian Science Foundation, https://rscf.ru/project/20-79-10285/.

Conflict of interest

The authors declare that they have no conflict of interest.

References

[1] J. Mayer, L.A. Giannuzzi, T. Kamino, J. Michael. MRS Bulletin, **32**, 400 (2007).

[2] P. Li, S. Chen, H. Dai, Z. Yang, Z. Chen, Y. Wang, Y. Chen, W. Peng, W. Shan, H. Duan. Nanoscale, **13**, 1529 (2021).

[3] F. Machalett, P. Seidel. Digital Encyclopedia of Applied Physics (N.Y., Wiley-VCH Verlag, 2019).

[4] J.A. Holguín-Lerma, T.K. Ng, B.S. Ooi. Appl. Phys. Express, **12**, 042007 (2019).

[5] M. Yoshida, M.D. Zoysa, K. Ishizaki, W. Kunishi, T. Inoue, K. Izumi, R. Hatsuda, S. Noda. J. Phys. Photonics, **3**, 022006 (2021).

[6] G.V. Voznyuk, I.N. Grigorenko, M.I. Mitrofanov, D.N. Nikolaev, M.N. Mizerov, V.P. Evtikhiev. Semiconductors, **54**, 1869 (2020).

[7] I.P. Soshnikov, N.A. Bert. Tech. Phys., **45** (9), 1201 (2000).

[8] W.J. Weber, Y. Zhang. Curr. Opin. Solid State Mater. Sci., **23** (4), 100757 (2019).

[9] G.V. Voznyuk, Y.V. Levitskii, M.I. Mitrofanov, M.N. Mizerov, D.N. Nikolayev, V.P. Evtikhiev. J. Phys.: Conf. Ser., **1038**, 012080 (2018).

[10] Y.V. Levitskii, M.I. Mitrofanov, G.V. Voznyuk, D.N. Nikolayev, M.N. Mizerov, V.P. Evtikhiev. Semiconductors, **53**, 1545 (2019).

[11] A. Azarov, V. Venkatachalapathy, P. Karaseov, A. Titov, K. Karabeshkin, A. Struchkov, A. Kuznetsov. Scientific Rep., **12**, 15366 (2022).

[12] N.A. Bert, K.Yu. Pogrebitskii, I.P. Soshnikov, Yu.N. Yur'ev. Zh. Tekh. Fiz., **62** (4), 163 (1992) (in Russian).

[13] N.P. Stepina, G.A. Kachurin. Fiz. Tekh. Poluprovodn., **17** (3), 449 (1983) (in Russian).